CHAPTER II

RESERVOIR PERFORMANCE

In the analysis of well performance, the accurate predictions should be made as to what will flow into the borehole from the reservoir. The flow into the well depends on the drawdown or pressure drop in the reservoir, $\bar{p}_R - p_{wf}$. The relationship between flow rate and pressure drop occurring in the porous medium can be very complex and depends on parameters such as rock properties, flow regime, fluid saturations in the rock, compressibilities of the flowing fluids, formation damage or stimulation, turbulence, and drive mechanism.

The relationship between well inflow rate and pressure drawdown has often been expressed in the form of a productivity index, J.

$$J = \frac{0.00708 k_o h}{\mu_o B_o \ln(0.472 r_e / r_w)} \qquad [2.1]$$

where k_o = oil permeability (md)

h = reservoir thickness (ft)

μ_o = oil viscosity (cp)

B_o = oil formation volume factor (RB/STB)

r_e = external boundary radius (ft)

r_w = wellbore radius (ft)

The inflow equation for oil can then be written as

$$q_o = J(\bar{p}_R - p_{wf}) \qquad [2.2]$$

or

$$J = \frac{q_o}{\bar{p}_R - p_{wf}} \qquad [2.3]$$

Solving for p_{wf} in terms of q_o reveals that a plot of p_{wf} versus q_o on cartesian coordinates results in a straight line having a slope of -1/J and an intercept of $\bar{p}_R$ at $q_o = 0$.

$$p_{wf} = \bar{p}_R - \frac{q_o}{J} \qquad [2.4]$$

This implies that the pressure function $f(p) = k_o/\mu_o B_o$ remains constant, which is seldom the case, as will be discussed further in following section.

The skin factor S' includes the effects of both turbulence and actual formation damage as:

$$S' = S + Dq \qquad [2.5]$$

where S = skin factor due to permeability change, and D = turbulence coefficient. The expression for the productivity index of an oil well, including skin effect, can be expressed as:

$$J = \frac{0.00708h}{\left(\bar{p}_R - p_{wf}\right)\left[\ln\left(0.472\frac{r_e}{r_w}\right) + S'\right]} \int_{p_{wf}}^{\bar{p}_R} \frac{k_o}{\mu_o B_o} dp \qquad [2.6]$$

From this expression, it can be observed that J will not be constant unless the pressure function is independent of pressure. The pressure function was defined in the term of $f(p_R)$.

$$f(p_R) = \frac{k_o}{\mu_o B_o} \qquad [2.7]$$

In this chapter, some of the factors that cause J to change are discussed.

2.1 Factor Affecting Inflow Performance

The inflow performance relationship (IPR) is the relationship between flow rate into the wellbore and wellbore flowing pressure, p_{wf}. The IPR is illustrated graphically by ploting p_{wf} versus q. If the IPR can be represented by a constant productivity index J, the plot will be linear, and the slope of the line drawn from $\bar{p}_R$ to p_{wf} will be -1/J, with intercepts of $p_{wf} = \bar{p}_R$ and $q = q_{max}$ at values of $q = 0$ and $p_{wf} = 0$, respectively as shown in Fig. 2.1.

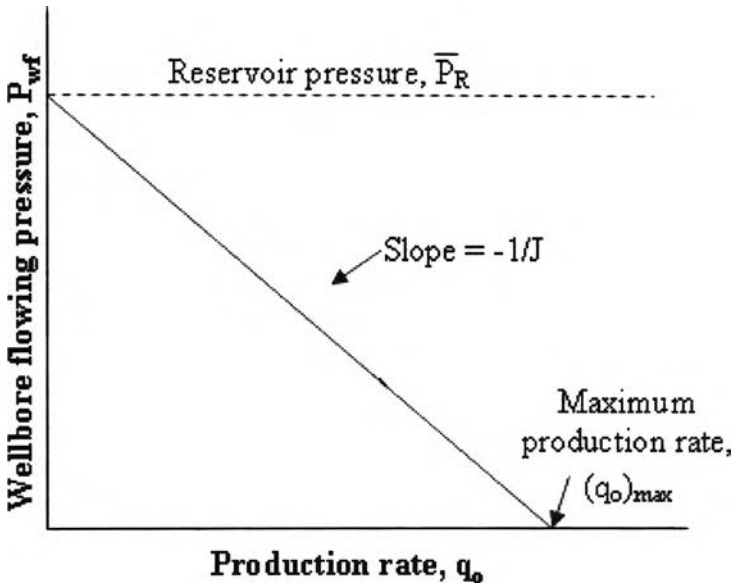

Figure 2.1: Inflow performance relationship with constant productivity index, J.

From the theoretical expression of J given in Eq. 2.6, it can be pointed out that changes occurring in some of the variables could cause J to change. If the value of J changes, the slope of the IPR plot will change, and a linear relationship between p_{wf} and q will no longer exist as shown in Fig 2.2. The principal factors affecting the IPR which are phase behavior of fluids in the reservoir, relative permeability, oil viscosity, oil formation volume factor, skin factor, and drive mechanism will be discussed in detail.

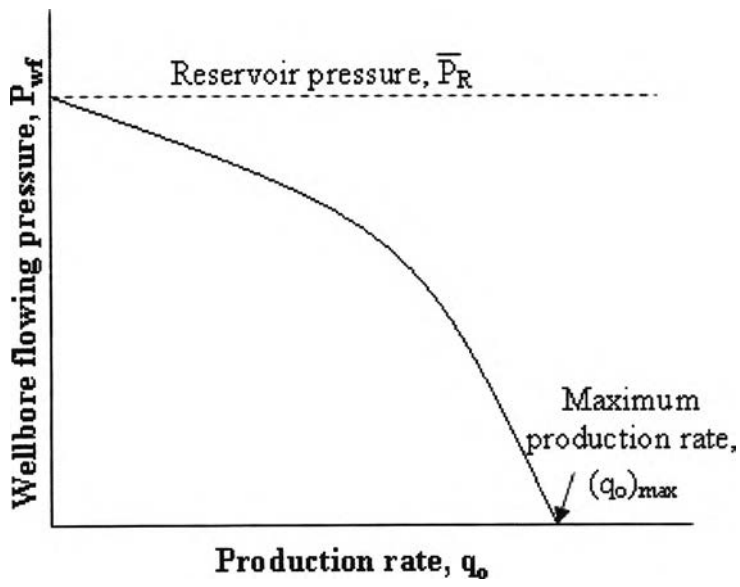

Figure 2.2: Inflow performance relationship with changing productivity index, J.

2.1.1 Phase Behavior of Fluids in the Reservoir

The concept of bubble point pressure and dew point pressure will be reviewed because of the importance of gas saturation on the relative permeability to oil. A typical pressure-temperature phase diagram for an oil reservoir is shown in Fig 2.3. The liquid, gas, and two-phase regions are shown, and the bubble point pressure is indicated as the pressure at which free gas first forms in the reservoir as pressure is reduced at constant reservoir temperature.

The reservoir fluid depicted in Fig. 2.3 is above the bubble point pressure, p_b, at initial reservoir pressure, $\overline{p}_{Ri}$, and, therefore, no free gas would exist anywhere in the reservoir. However, if the pressure at any point in the reservoir drops below p_b, free gas will form and k_{ro} will be reduced. Therefore, if a well is produced at below bubble point pressure, k_{ro} and therefore J will decrease. This situation can occur even though $\overline{p}_R$ may be well above p_b.

As pressure depletion in the reservoir occurs, $\overline{p}_R$ will likely drop below p_b, and free gas will exist throughout the reservoir.

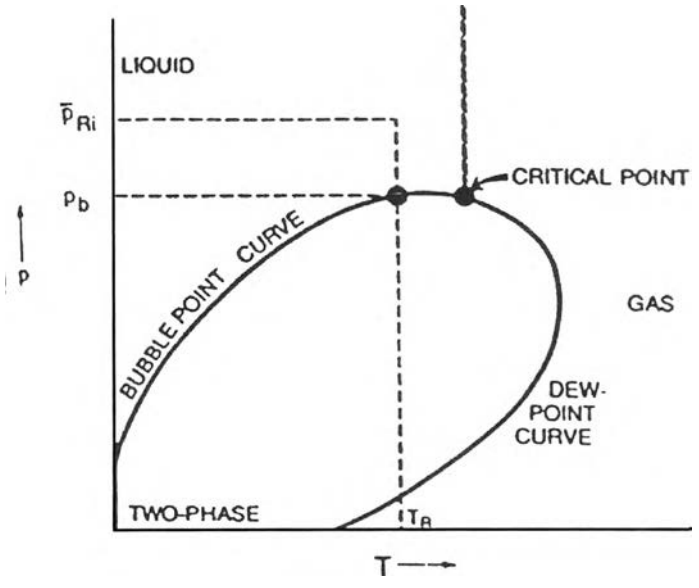

Figure 2.3: Oil reservoir phase diagram.

2.1.2 Relative Permeability

As free gas forms in the pores of a reservoir rock, the ability of the liquid phase to flow is decreased. Even though the gas saturation may not be great enough to allow gas to flow, the space occupied by the gas reduces the effective flow area for the liquids. The behaviors of the relative permeability to oil and the relative permeability to gas as a function of liquid saturation are shown in Fig. 2.4. As the gas saturation increases, the gas relative permeability increases, resulting in the ability of the gas flow more easily. On the other hand, the oil will flow less due to less oil relative permeability. When the gas saturation decreases, the relative permeability to oil increases, enabling the oil to flow more and gas to flow less.

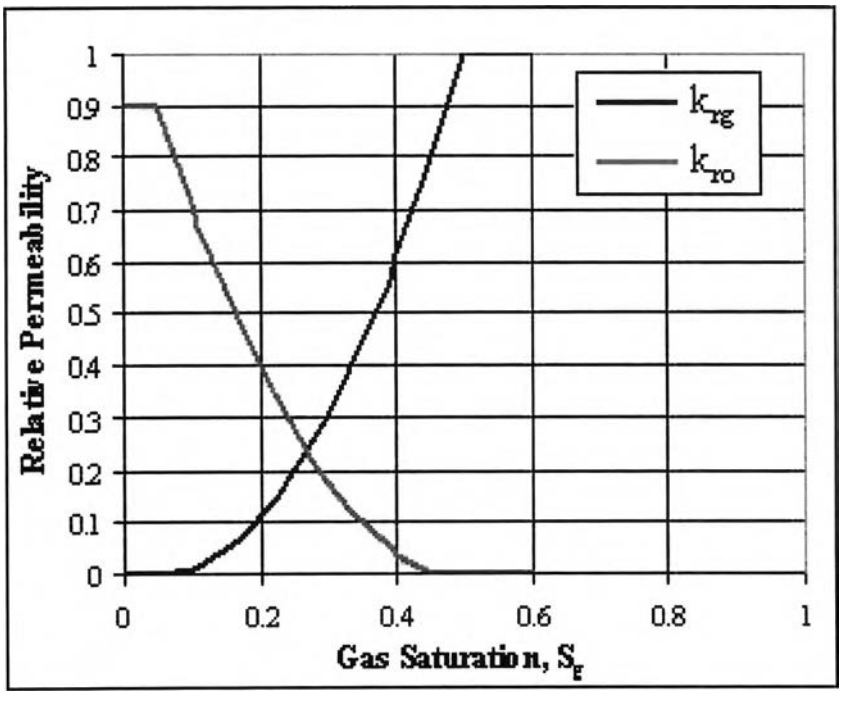

Figure 2.4: Gas-oil relative permeability.

2.1.3 Oil Viscosity

Fig. 2.5 illustrates qualitatively the behavior of μ_o versus pressure at constant temperature. The viscosity of oil saturated with gas at constant temperature will decrease as the pressure decreases from the initial pressure to the bubble point pressure. Below p_b, the oil viscosity, μ_o, will increase as gas comes out of solution leaving the heavier molecules in the liquid phase. When viscosity of oil increases, J will decrease, which means that the slope of IPR curve will increase after the reservoir pressure falls below the bubble point pressure.

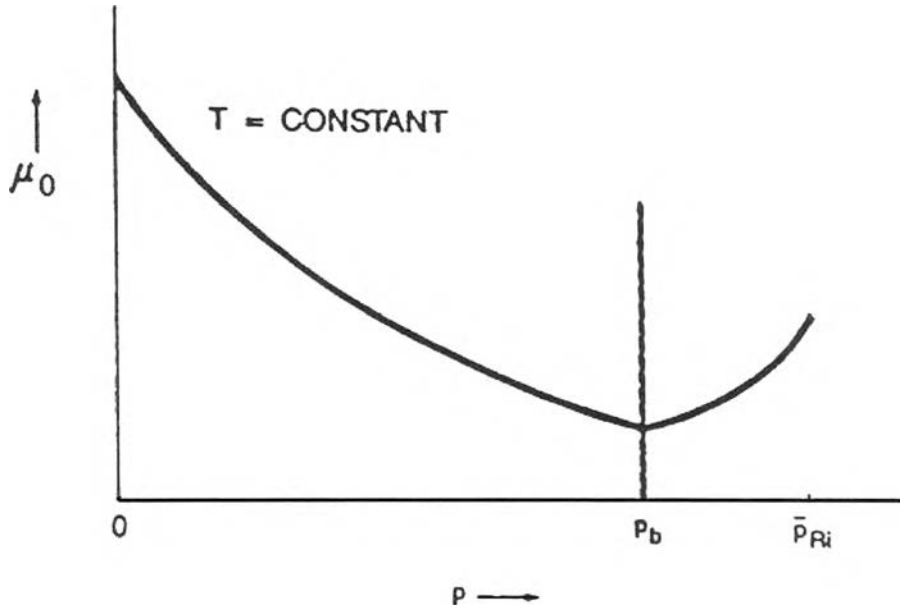

Figure 2.5: Oil viscosity behavior.

2.1.4 Oil Formation Volume Factor

As pressure is decreased on a liquid, the liquid will expand. When the bubble point pressure is reached, gas coming out of solution will cause the oil to shrink. The behavior of B_o versus p at constant temperature is shown graphically in Fig. 2.6. When B_o decreases at pressures below the bubble point pressure, J will increase and the slope of IPR curve will decrease.

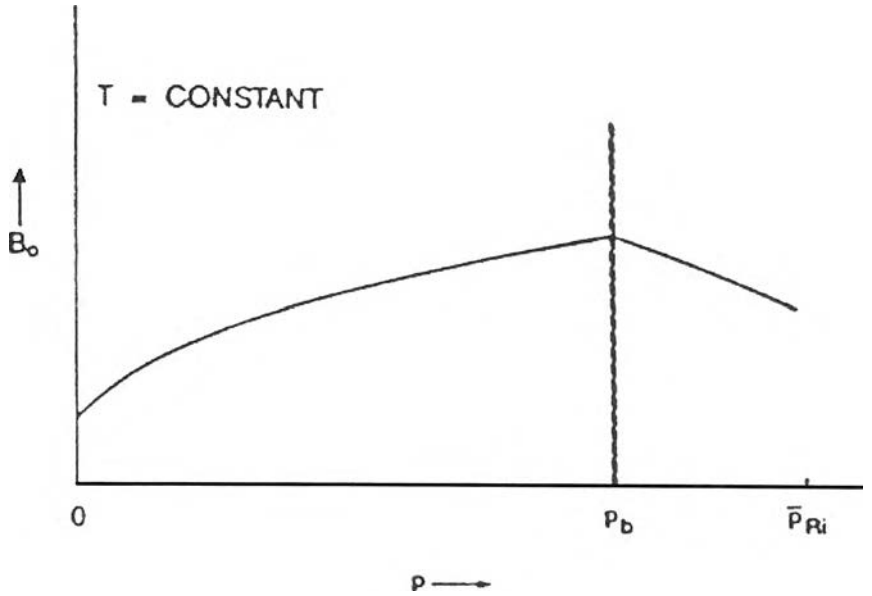

Figure 2.6: Oil formation volume factor behavior.

2.1.5 Skin Factor

The skin factor *S'* is positive for damage, negative for improvement, and zero for no change in permeability. The absolute permeability, *k*, can be either increased around the wellbore by well stimulation resulting in a negative skin or decrease by formation damage such as clay swelling or pore plugging resulting in a positive skin. The changing of skin factor is directly related to permeability and q_o. From Eq 2.6, when skin factor increases, *J* will decrease. Therefore, the slope of IPR curve increases. The effect of *S'* on the pressure profile for an oil reservoir are illustrated in Fig. 2.7.When permeability is increased around the wellbore by well stimulation, the wellbore flowing pressure increases. Then, the productivity index will increase. On the other hand, the well flowing pressure decreases when the permeability around the wellbore is decreased, resulting in a lower productivity index.

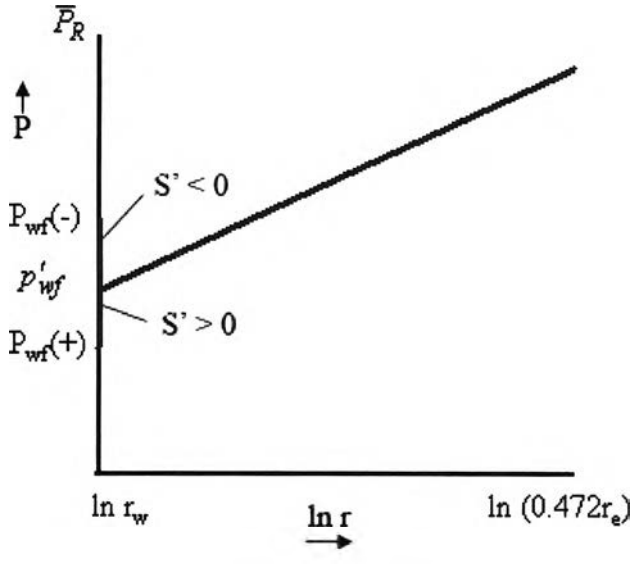

Figure 2.7: Effects of skin factor.

2.1.6 Drive Mechanisms

The source of pressure energy causing the oil and gas to flow into the wellbore has a substantial effect on both the performance of the reservoir and the total production. General descriptions of the three basic types of drive mechanisms are presented. The behavior of reservoir pressure, $\bar{p}_R$, the pressure function, $f(\bar{p}_R)$, evaluated at $p = \bar{p}_R$, and surface producing gas/oil ratio, R, versus cumulative recovery, N_p, is presented graphically for each drive mechanism.

A. Solution Gas Drive. A solution-gas-drive reservoir is closed from any outside source of energy such as water encroachment. Its pressure is initially above the bubble point pressure; therefore, no free gas exists. The only source of material to replace the produced fluids is the expansion of the fluids remaining in the reservoir. Some small but usually negligible expansion of the connate water and rock may also occur.

The reservoir pressure declines rapidly with production until $\bar{p}_R = p_b$ since only the oil is expanding to replace the produced fluids. The producing gas/oil ratio will be

constant at $R = R_{si}$ during this period. Also, since no free gas exists in the reservoir, the pressure function, $f(\bar{p}_R)$, will remain fairly constant.

Once $\bar{p}_R$ declines below p_b, free gas will be available and expand, and $\bar{p}_R$ will decline less rapidly. However, as soon as the gas saturation exceeds the critical gas saturation, R will increase rapidly, further depleting the reservoir energy. As abandonment conditions are reached, R will begin to decrease because most of the gas has been produced, and, at low reservoir pressures, the reservoir gas volumes are more nearly equal to the standard surface volumes.

Recovery efficiency at abandonment conditions will range between 5% and 30% of original oil in place. However, in most cases, some type of pressure maintenance is applied to supplement the reservoir energy and increase recovery. Typical dissolved-gas drive performance under primary depletion is shown in Fig. 2.8.

Therefore, slope of IPR will increase after the reservoir pressure decreases below the bubble point pressure because when the pressure function $f(p_R)$ rapidly decreases. As a result, the productivity index will decrease.

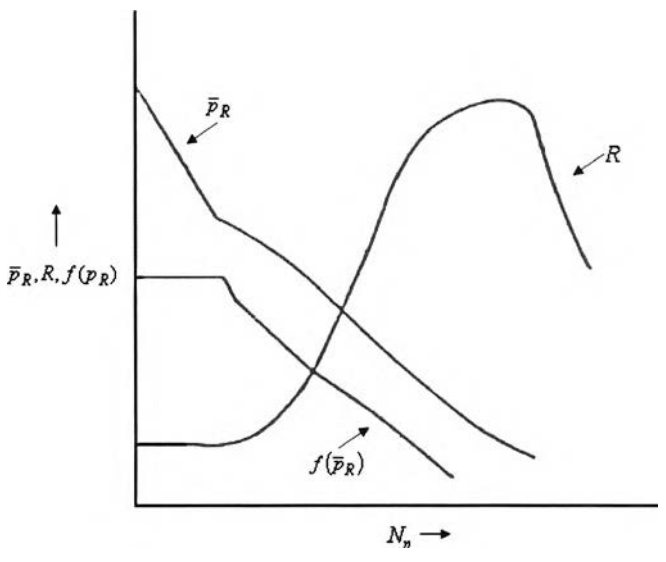

Figure 2.8: Dissolved gas drive performance[6].

B. Gas Cap Drive. A gas cap drive reservoir is also closed from any outside source of energy but the oil is saturated with gas at its initial pressure. Therefore, free gas will exist. As oil is produced, the gas cap will expand and help to maintain the reservoir pressure. Also, as the reservoir pressure declines as a result of production, gas will evolve from the saturated oil.

The reservoir pressure of gas-cap drive reservoir will decline more slowly than that of a dissolved-gas drive. However, as the free gas cap expands, some of the upstructure wells will produce at high gas/oil ratios. The recovery efficiency may be increased by re-injecting the produced gas into the gas cap. Also, the effects of gravity may increase recovery, especially if producing rates are low and the formation has an appreciable dip. Typical performance for a gas cap drive reservoir is shown in Fig. 2.9.

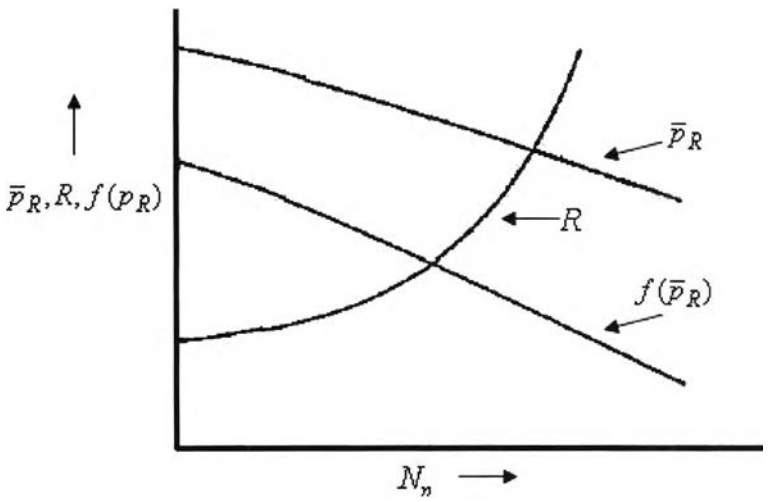

Figure 2.9: Gas cap drive performance[6].

As depletion proceeds below the bubble point pressure a solution-gas drive reservoir, the productivity of a typical well decreases primarily because the reservoir pressure is lower and because increasing gas saturation causes greater resistance to oil flow. The result is a progressive deterioration of the IPR's, typified by the IPR curves in Fig. 2.10.

C. Water Drive. In a water-drive reservoir, the oil zone is in contact with an aquifer that can supply the material to replace the produced oil and gas. The water that encroaches may come from expansion of the water only, or the aquifer could be connected to a surface outcrop. The oil may be undersaturated initially, but if the pressure declines below the bubblepoint, free gas will form and the dissolved-gas drive mechanism will also contribute to the energy for production.

The recovery factor to be expected from a water-drive reservoir may vary from 35% to 75% of the initial oil in place. If the producing rate is low enough to allow water to move in as rapidly as oil and gas are produced or if the water drive is supplemented by water injection, recovery may be even higher. If the reservoir pressure remains above the bubblepoint, no free gas will form, and the pressure function, based on $\bar{p}_R$, will remain fairly constant, resulting in a fairly constant productivity index. The performance of a strong water drive is illustrated in Fig 2.11.

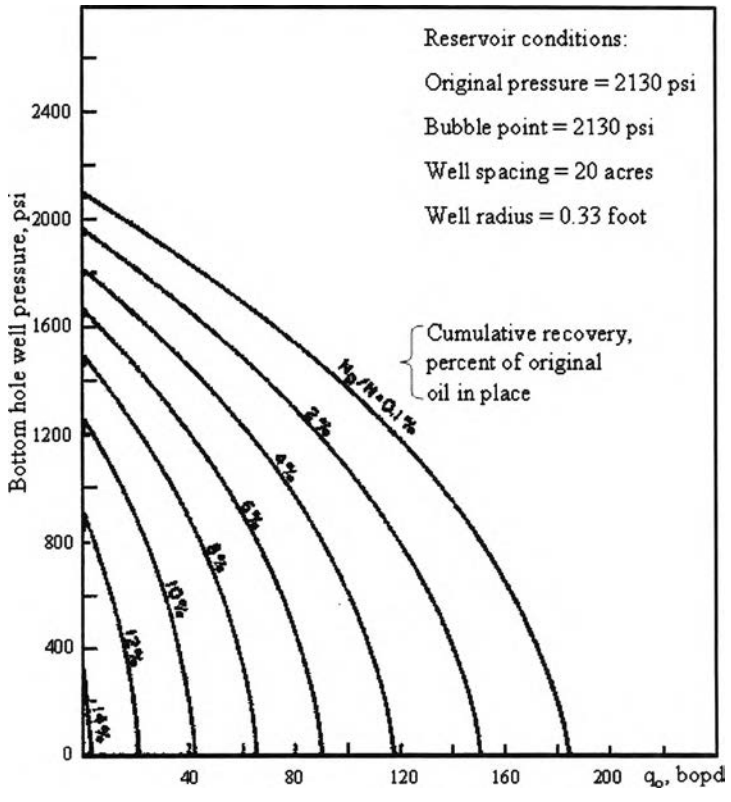

Figure 2.10: Computer-calculated inflow performance relationships for a solution-gas drive reservoir[2].

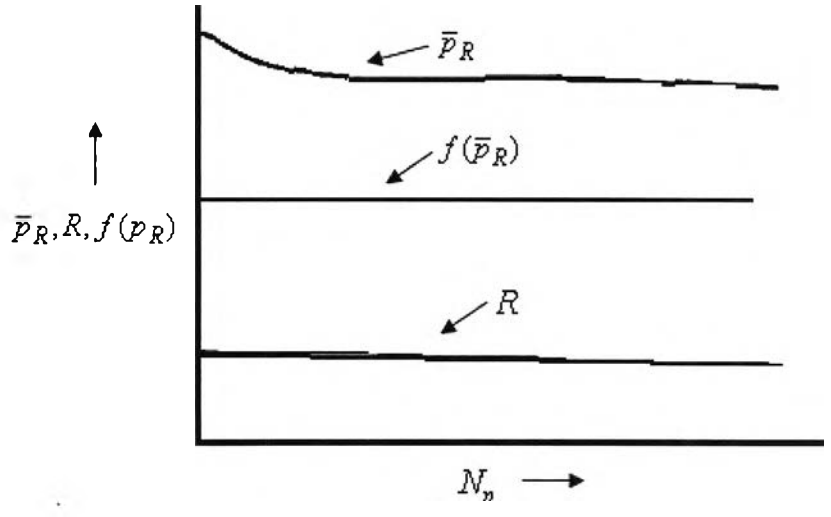

Figure 2.11: Water drive performance[6].

D. Combination Drive. In many cases, an oil reservoir is both saturated and in contact with an aquifer. In this case, all three of the previously described mechanisms may be contributing to the reservoir drive. As oil is produced, both the gas cap and aquifer will expand, and the gas/oil contact will drop as the oil/water contact rises, which can cause complex production problems. It is impossible to generalize on the expected recovery and performance of a combination-drive reservoir because of a wide variation in gas cap and aquifer sizes. The drive mechanism may be supplemented by both gas and water injection.

2.2 Empirical Correlations for Inflow Performance Relationship

The early investigation of performance of oil wells was derived from Darcy's law (1856) in radial coordinates as

$$q = \frac{kA}{\mu}\frac{dp}{dr} \qquad [2.8]$$

where A = an area perpendicular to the flow direction at a distance r and is given by $A = 2\pi rh$. This expression assumes a single-phase fluid flowing and saturating the

reservoir. It then gives a straight-line relationship as shown in Fig. 2.12. But the relationship of straight-line has limitation when applied to two phases.

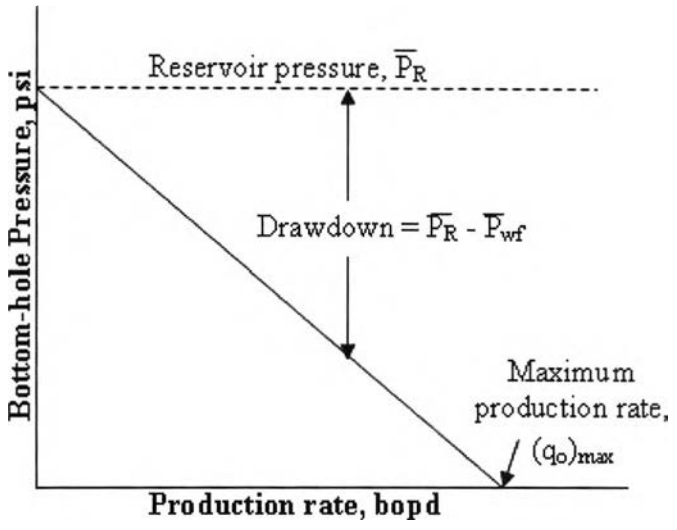

Figure 2.12: Straight-line inflow performance relationship.

Later, many empirical expansions for IPR have been developed such as (1) Vogel[1], (2) Fetkovich[2], (3) Jones, Blount and Glaze[3], (4) Klines and Majcher[7], (5) Sukarno[8], (6) Evinger and Muskat[9] etc.

2.2.1 Vogel Method

In 1968, Vogel[1] presented an empirical equation to estimate two-phase inflow performance relationship in vertical wells. The study dealt with several hypothetical reservoirs including those with widely differing oil characteristics, relative permeability characteristics, well spacings, and skin factors. The final equation for Vogel's method was based on calculations made for 21 reservoir conditions.

Although the method was proposed for saturated, dissolved-gas-drive reservoirs only, it has been found to apply for any reservoir in which gas saturation increases as the pressure decreases.

The Vogel method was developed by using the reservoir model proposed by Weller[5] to generate IPR's for a wide range of conditions. Weller describes the pressure gradient as

$$\frac{\partial p}{\partial r} = 141.2 \frac{\mu_o q_o B_o}{r k k_{ro} h} \left(\frac{r_e^2 - r^2}{r_e^2 - r_w^2} \right) \qquad [2.9]$$

where r_e = external boundary radius (ft)

r_w = wellbore radius (ft)

r = radius of investigation (ft)

μ_o = oil viscosity (cp)

B_o = oil formation volume factor (RB/STB)

k_{ro} = relative oil permeability

The oil saturation at any time and location can be estimated from

$$\frac{S_o}{B_o} = \frac{S_{oi}}{B_{oi}} \left(1 - \frac{N_p - N_{pt}}{N} \right) - 92.6 \frac{q_o c_{oi} \mu_{oi}}{k_{oi} h} \ln \frac{r_d r_w}{r_e + r_w} \qquad [2.10]$$

where N_p = cumulative oil production (STB)

N_{pt} = cumulative oil producing during transient period (STB)

r_d = external drainage area (ft)

c_{oi} = initial oil compressibility (1/psi)

μ_{oi} = initial oil viscosity (cp)

k_{oi} = initial oil permeability (cp)

The fractional recovery, N_p/N, is calculated by the Muskat[10] method. The skin effect was viewed as a zone of finite width altered permeability and defined by Hawkins[11] as

$$S = \left(\frac{k}{k_s} - 1 \right) \ln \left(\frac{r_s}{r_w} \right) \qquad [2.11]$$

where k_s = altered permeability from skin effect (md)

r_s = damage radius (ft)

Vogel then replotted the IPR's as reduced or dimensionless pressure versus dimensionless flow rate. The dimensionless pressure is defined as the wellbore flowing pressure divided by average reservoir pressure, $p_{wf}/\bar{p}_R$. The dimensionless flow rate is defined as the flow rate that would result from the value of p_{wf} being considered divided by the flow rate that would result from a zero wellbore pressure, that is $\frac{q_o}{q_{o(\max)}}$. It was found that the general shape of the dimensionless IPR is similar for all of the conditions studied.

After plotting dimensionless IPR curves for all the cases considered, this empirical equation is given as

$$\frac{q_o}{q_{o,\max}} = 1 - 0.2\left(\frac{p_{wf}}{\bar{p}_R}\right) - 0.8\left(\frac{p_{wf}}{\bar{p}_R}\right)^2 \qquad [2.12]$$

where p_{wf} = flowing bottom hole pressure (psi)

$\bar{p}_R$ = average reservoir pressure (psi)

$q_{o.max}$ = oil production rate at the maximum drawdown
or at zero bottomhole flowing pressure (BOPD)

q_o = oil flow rate (BOPD)

Vogel pointed out that in most applications the error in the predicted inflow rate should be less than 10%, but could increase to 20% during the final stages of depletion. It has also been shown that Vogel's method can be applied to wells producing water along with the oil and gas since the increased gas saturation will also reduce the permeability to water. The ratio $\frac{q_o}{q_{o(\max)}}$ can be replaced by $\frac{q_L}{q_{L(\max)}}$ where q_L= liquid production rate = $q_o + q_w$. This has been proven to be valid for wells producing at water cuts as high as 97%.

2.2.2 Fetkovich Method

Fetkovich[2] proposed a method for calculating the oil performance for oil wells using the same type of equation that has been used for analyzing gas wells for many years. The procedure was verified by analyzing flow-after-flow and isochronal tests conducted in reservoirs with permeabilities ranging from 6 md to greater than 1,000 md. Conditions in the reservoirs ranged from highly undersaturated to saturated at initial pressure and to a partially depleted field with a gas saturation above the critical value.

The Fetkovich[2] equation expresses the relationship between oil flow rate (q_o), average reservoir pressure ($\bar{p}_R$), and flowing bottomhole pressure (p_{wf}) by

$$q_o = J(\bar{p}_R^{\,2} - p_{wf}^2)^n \qquad [2.13]$$

where q_o = producing rate (BOPD)

J = flow coefficient

n = exponent coefficient

The changing of coefficient J and n are depending on well characteristics. In 1973, the experiment of 40 oil well back-pressure curves of Fetkovich[2] found that the exponent n lies between 0.568 and 1.000. The flow constant, J, was varied according to

$$J_2 = J_1(p_{r2} / p_{r1}) \qquad [2.14]$$

where J_1 = flow constant at current reservoir pressure, p_{r1},

J_2 = flow constant at a future reservoir pressure, p_{r2}

From a multipoint flow test, the variable n and J can be estimated and used for future maximum flow rate by

$$(q_o)_{max} = J_2 (p_{r2}^2)^n \qquad [2.15]$$

The applicability of Eq. 2.12 to oil well analysis was justified by writing Darcy's equation as:

$$q = \frac{0.00708kh}{\ln\left(0.472\frac{r_e}{r_w}\right) + S'} \int_{P_{wf}}^{\bar{P}_R} f(p)dp \qquad [2.16]$$

The pressure function, *f(p),* was defined as in Eq. 2.7. For an undersaturated reservoir, the integral is evaluated over two regions as:

$$q_o = J' \int_{p_{wf}}^{p_b} f_1(p)dp + J' \int_{p_b}^{\bar{p}_r} f_2(p)dp \qquad [2.17]$$

where

$$J' = \frac{0.00708kh}{\ln\left(\frac{0.472r_e}{r_w}\right) + S'} \qquad [2.18]$$

It was assumed that for $p>p_b$, k_{ro} is equal to one and that μ_o and B_o could be considered constant at $\bar{p} = \frac{\bar{p}_R + p_b}{2}$. It was also assumed that for $p < p_b$, $f(p)$ could be expressed as a linear function of pressure, that is

$$f_1(p) = ap + b \qquad [2.19]$$

Making these substitutions into Eq. 2.15 and integrating gives:

$$q_o = J_1 (p_b^2 - p_{wf}^2) + J_2 (\bar{p}_R - p_b) \qquad [2.20]$$

Once values for J and n are determined from test data, Eq. 2.12 can be used to generate a complete IPR. As there are two unknowns in Eq. 2.12, at least two tests are required to evaluate J and n, assuming $\bar{p}_R$ is known. However, in testing gas wells it has been customary to use at least four flow rates to determine J and n because of the possibility of errors. This is also recommended for oil well testing.

By taking log on both sides of Eq. 2.12 and solving for log $(\bar{p}_R^2 - p_{wf}^2)$, the expression can be written as

$$\log\left(\bar{p}_R^2 - p_{wf}^2\right) = \frac{1}{n}\log q_o - \frac{1}{n}\log J \qquad [2.21]$$

A plot of $\bar{p}_R^2 - p_{wf}^2$ versus q_o on log-log scales will result in a straight line having a slope of 1/n and an intercept of $q_o = J$ at log ($\bar{p}_R^2 - p_{wf}^2$) = *1*. The value of J can also be calculated using any point on the linear plot once n has been determined. That is

$$J = \frac{q_o}{\left(\bar{p}_R^2 - p_{wf}^2\right)^n} \qquad [2.22]$$

Deliverability Test

Deliverability testing[12] is a method to predict the capability of a gas well to deliver against a flowing bottom-hole pressure. It is also useful for reservoir systems operating below the bubble point when fluid properties and relative permeabilities vary with distance from the well. Oil flow rate (at surface conditions) has been empirically related to flowing bottom-hole pressure and average reservoir pressure by Eq. 2.13.

Three types of deliverability tests are the flow-after-flow test, isochronal test, and modified isochronal test. Fig. 2.13 demonstrates the rate and pressure behavior of a flow-after-flow test. The well is produced at rate q_1 until the pressure stabilizes at p_{wf1}. Then, the rate is changed to q_2 until the pressure stabilizes at p_{wf2}, and so on. Normally, four rates are run but any number greater than three may be used. Flow rate may be either increased or decreased. The disadvantage of the flow-after-flow test is that each rate must remain constant until the pressure stabilizes. The time required may be estimated from

$$t_s = \frac{380\phi\mu_o C_t A}{k_o} \qquad [2.23]$$

where t_s = stabilization time (hrs)

ϕ = a porosity

c_t = total fluid compressibility (psi^{-1})

A = drainage area (ft^2)

k_o = permeability to oil (md)

μ_o = oil viscosity (cp)

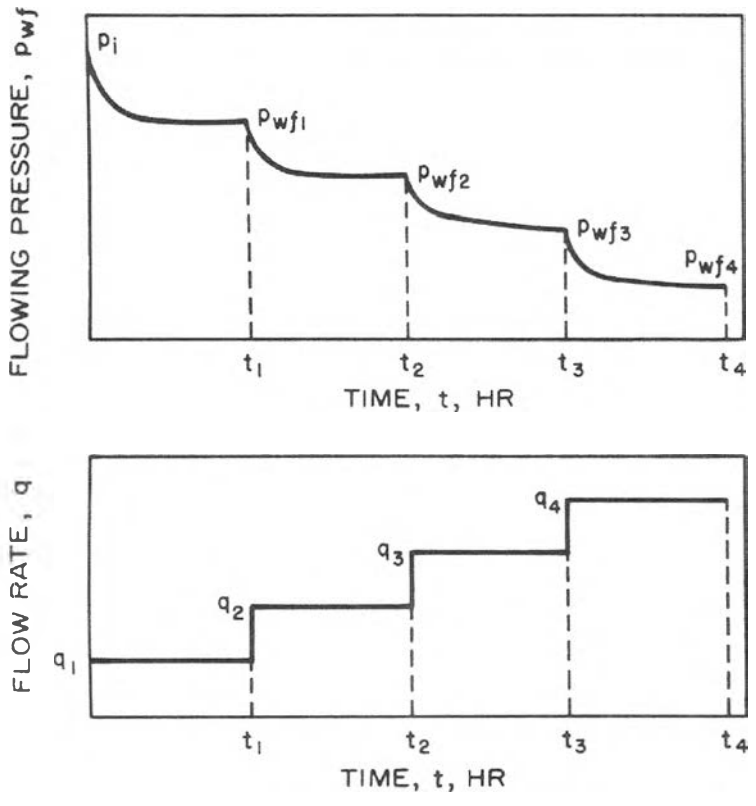

Figure 2.13: Pressure-rate history for a flow-after-flow test[12].

From systems that are large or have low permeability, stabilization time can be very long. To avoid this problem, Cullender[13] proposed the isochronal flow test for gas wells as shown in Fig. 2.14. The procedure for conducting an isochronal test is

a. Starting at a shut-in condition, open the well on a constant production rate and measure p_{wf}. The total production period may be less than the stabilization time.
b. Shut the well in and allow the pressure to build up to $\overline{p}_R$.
c. Open the well on another producing rate and measure the pressure at the same time interval.
d. Shut the well in again until $p_{ws} = \overline{p}_R$.
e. Repeat this procedure for several rates.

The values of $\bar{p}_R^2 - p_{wf}^2$ determine at specific time periods are plotted versus q_o on a log-log plot, and n is obtained from the inverse of the slope of the line drawn through the data. To determine a value for J, one flow period must be a stabilized flow period.

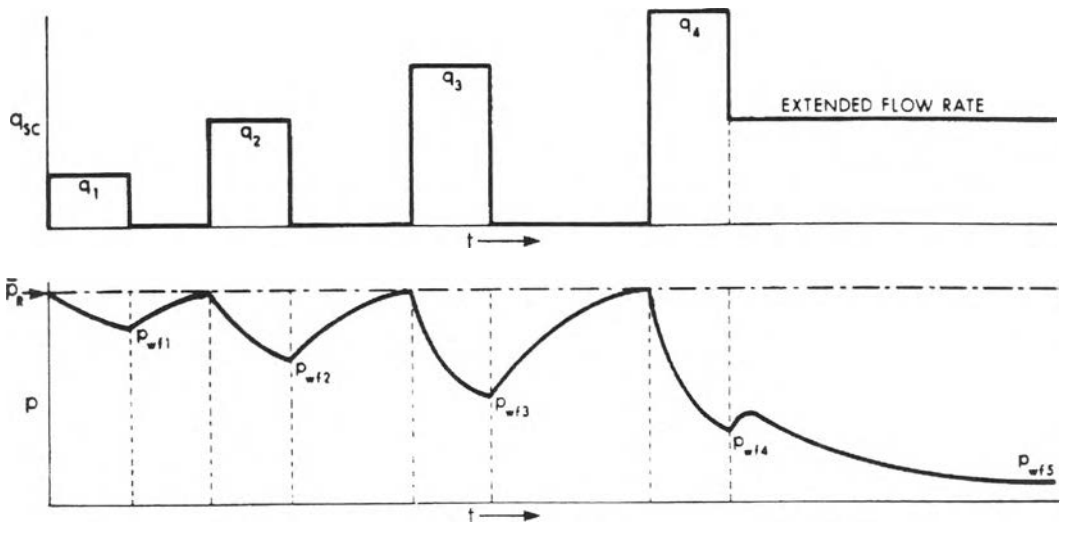

Figure 2.14: Pressure-rate for an isochronal flow test[12].

A shortened version, the modified isochronal test, was suggested later and generally preferred. Fig 2.15 illustrates schematic of flowrate and pressure for a modified isochronal flow test. The well is produced at rate q_1 for duration t_1 and the final flowing pressure, p_{wf1}, is observed. Then, the well is shut-in for the same duration, t_1, and the shut-in pressure, p_{ws2}, is observed. Then, repeat the procedure for rates q_2, q_3, q_4, etc. The well is usually produced to a stabilized pressure at the final rate so one stabilized pressure point, $(p_{wf})_{pss}$, is available.

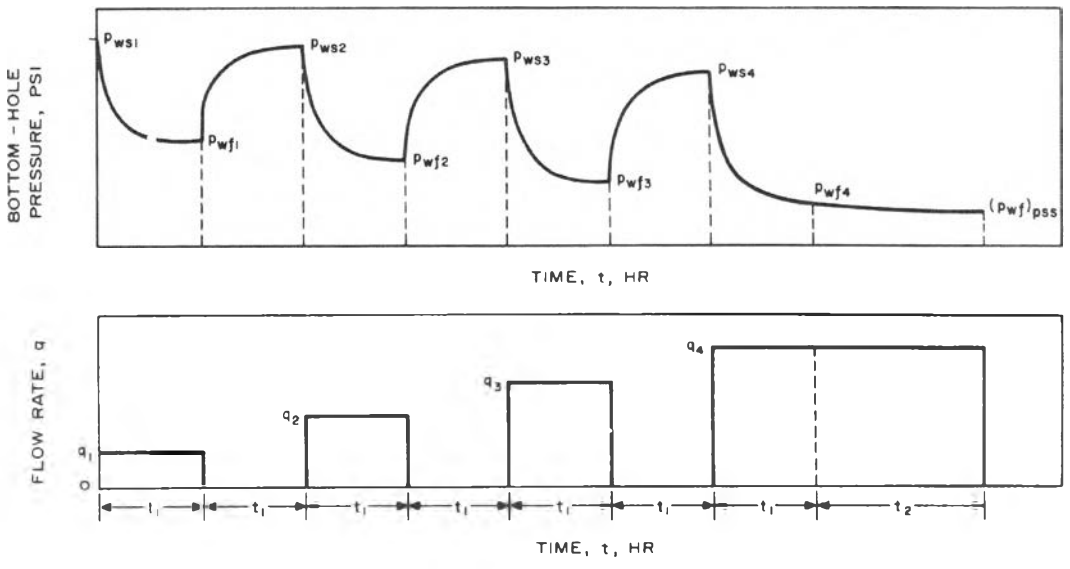

Figure 2.15: Pressure-rate for a modified isochronal flow test[12].

In the analysis, the parameters J and n are constant when stabilization has been reached. The analysis method of modified isochronal deliverability test is done by plotting log $(p^2 - p_{wf}^2)$ vs. log q. This plot will give a straight line as shown in Fig. 2.16 with slope $1/n$. The location of the line depends on the flow period duration. Thus, in normal analysis, the points from the four rates define the straight line, and the single stabilized point defines location of the stabilized deliverability curve. The stabilized deliverability curve may be entered at set values of $\left(\bar{p}^2 - p_{wf}^2\right)$ to estimate the well deliverability (flow rate) at a given drawdown. Alternatively, the plot (Fig. 2.16) may be used to estimate J and n, and the flow rate may be estimated from Eq. 2.12.

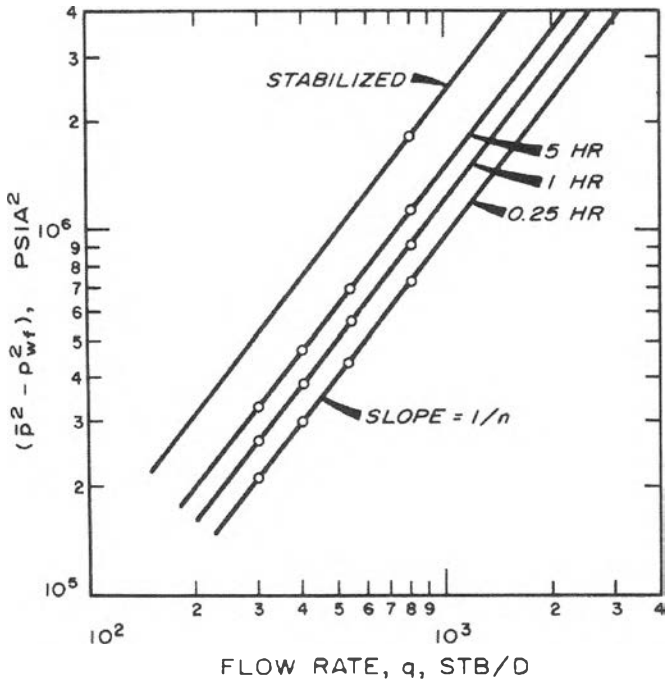

Figure 2.16: Schematic of example of a modified-isochronal test data plot[12].

The type of test to choose depends on the stabilization time of the well, which is a function of the reservoir permeability, porosity, reservoir size, fluid viscosity, and fluid compressibility. If a well stabilizes fairly rapidly, a conventional flow-after-flow test can be conducted. For tight reservoirs, an isochronal test may be preferred. For wells with very long stabilization times, a modified isochronal test may be more practical. The stabilization time for a well in the center of a circular or square drainage area can be estimated from Eq. 2.23.

2.2.3 Jones, Blount, and Glaze Method

Jones, Blount, and Glaze presented a method to analyze well completion efficiency and to isolate the rate dependent component of the total pressure drawdown. In 1976, the paper [3] was published and discussed the effects of turbulence or non-Darcy flow on well performance. When including turbulence term in the evaluation, the equation can expressed as

$$\bar{p}_R - p_{wf} = Aq_o + Bq_o^2 \qquad [2.24]$$

where $$A = \frac{141.2\mu_o B_o}{k_o h}\left[\ln\left(\frac{0.472r_e}{r_w}\right) + S\right]$$

$$B = \frac{2.3\times10^{-14}\beta B_o^2 \rho_o}{h^2 r_w} = \frac{141.2\mu_o B_o}{k_o h} D$$

ρ_o = oil density evaluated at T_R

β = velocity coefficient (ft^{-1})

The contribution to the pressure drawdown due to laminar or Darcy flow is expressed as Aq_o while the non-Darcy or turbulent contribution is expressed as Bq_o^2. Dividing Eq 2.24 by q_o gives

$$\frac{\bar{p}_R - p_{wf}}{q_o} = A + Bq_o \qquad [2.25]$$

The plot of $\frac{\bar{p}_R - p_{wf}}{q_o}$ versus q_o on cartesian coordinates should yield a straight line of slope B and intercept A as q_o approaches zero. Once A and B are determined, a complete IPR can be constructed using Eq. 2.24 or Eq. 2.25. At least two stabilized tests are required to evaluate A and B, but usually more tests will be used to smooth out the the effects of errors in measurements.

2.3 Predicting Future Inflow Performance Relationship

As the pressure in an oil reservoir declines from depletion, the ability of the reservoir to transport oil will also decline. This is caused by the decrease in the pressure function as relative permeability to oil is decreased due to increasing gas saturation. Planning the development of a reservoir with respect to sizing equipment and planning for artificial lift as well as evaluating the project from an economics standpoint requires the ability to predict reservoir performance in the future. The effect of depletion was discussed previously, and in this section several methods to quantify this effect will be presented.

2.3.1 Fetkovich Method

The method proposed by Fetkovich[2] to construct future IPR's consists of adjusting the flow coefficient J in Eq. 2.12 for changes in $f(\bar{p}_R)$. He assumed that $f(\bar{p}_R)$ was a linear function of $\bar{p}_R$, and, therefore the value of J can be adjusted as.

$$J_F = J_P(\bar{p}_{RF} / \bar{p}_{RP}) \qquad [2.26]$$

where J_P = flow coefficient at present time

$\bar{p}_{RP}$ = reservoir pressure at present time

J_F = flow coefficient at future time

$\bar{p}_{RF}$ = reservoir pressure at future time

Fetkovich assumed that the value of the exponent n would not change. Future IPR's can thus be generated from

$$q_{o(F)} = J_P(\bar{p}_{RF} / \bar{p}_{RP})(\bar{p}_{RF}^2 - \bar{p}_{wf}^2)^n \qquad [2.27]$$

2.3.2 Klines and Clark Method

Klines and Clark[4] published a procedure that can be used to predict the new $q_{o(max)}$ at future reservoir pressures. To develop a general equation that could be used to predict future inflow performance for any solution-gas-drive reservoirs, IPR curves were simulated for wells producing from 21 theoretical reservoirs with Weller method by Eq. 2.8 and 2.9. The data used in the simulations contained a wide range of rock and fluid properties, relative permeability characteristics, and skin effects. For each parameter, runs were made for eight different values. For each data case, curves were generated for eight depletion stages. These combinations of conditions resulted in the generation of 1,344 IPR curves with 19,492 total data points.

Fetkovich-type isochronal plots were generated for each of the case to estimate the flow exponent n and PI coefficient J by regression techniques. Because the absolute values for n and J varied greatly from case to case, these relationships had to be converted to a dimensionless form related to values at the bubble point pressure. Then, a

relationship between dimensionless n/n_b, dimensionless J/J_b, and dimensionless pressure p_r/p_b could be made. The third-order polynomial fit was generated with the dimensionless n/n_b and J/J_b values, and the equations that describe the trends are

$$\frac{n}{n_b} = 1 + 0.0577\left(1 - \frac{p_r}{p_b}\right) - 0.2459\left(1 - \frac{p_r}{p_b}\right)^2 + 0.5030\left(1 - \frac{p_r}{p_b}\right)^3 \qquad [2.28]$$

and

$$\frac{J}{J_b} = 1 - 3.5718\left(1 - \frac{p_r}{p_b}\right) + 4.7981\left(1 - \frac{p_r}{p_b}\right)^2 - 2.3066\left(1 - \frac{p_r}{p_b}\right)^3 \qquad [2.29]$$

With this equation, n and J values can be estimated easily at any given pressure. To predict future maximum oil deliverability as a function of J and n, the Fetkovich Eq. 2.12 for deliverability can be used at any given pressure. By assuming a flowing BHP of zero, the AOF potential at any reservoir pressure below the bubble point can be estimated.

2.3.3 Standing Method

Standing[14] published a procedure that can be used to predict the decline in the value of $q_{o(max)}$ as gas saturation in the reservoir increases from depletion. Vogel's eq. 2.11 can be rearranged to yield

$$\frac{q_o}{q_{o(\max)}} = \left(1 - \frac{p_{wf}}{\bar{p}_R}\right)\left(1 + 0.8\frac{p_{wf}}{\bar{p}_R}\right) \qquad [2.30]$$

Substituting the expression for the productivity index Eq. 2.3 into Eq. 2.26 and rearranging gives

$$J = \frac{q_{o(\max)}}{\bar{p}_R}\left(1 + 0.8\frac{p_{wf}}{\bar{p}_R}\right) \qquad [2.31]$$

Standing then defined a "zero drawdown" productivity index as:

$$J^* = \lim_{p_{wf} \to \bar{p}_R} J = \frac{1.8 q_{o(\max)}}{\bar{p}_R} \qquad [2.32]$$

or

$$q_{o(\max)} = \frac{J^* \bar{p}_R}{1.8} \qquad [2.33]$$

If the change of J^* with depletion can be predicted, then the change of $q_{o(max)}$ can be calculated. Standing observed that another definition of J^* is

$$J^* = \frac{0.00708kh}{\ln\left(\frac{0.472r_e}{r_w}\right)}(f(\bar{p}_R)) \qquad [2.34]$$

The relationship between the present or real time J^* and some future time value of J^* can be expressed as

$$\frac{J_F^*}{J_P^*} = \frac{f(\bar{p}_{RF})}{f(\bar{p}_{RP})} \qquad [2.35]$$

where J_F^* = value of J^* when $\bar{p}_{RP}$ has declined to $\bar{p}_{RF}$ and J_P^* = value of J^* at the present reservoir pressure. Combining Eq. 2.35 and 2.32 gives a relationship between $q_{o(max)P}$ and $q_{o(max)F}$ as

$$q_{o(\max)F} = q_{o(\max)P}\left[\frac{\bar{p}_{RF}f(\bar{p}_{RF})}{\bar{p}_{RF}f(\bar{p}_{RP})}\right] \qquad [2.36]$$

Once a value of $q_{o(max)}$ is determined from a well test conducted at the present or real time, future values of $q_{o(max)}$ can be predicted if the value of the pressure function can be predicted at $\bar{p}_{RF}$. The oil saturation as a function of $\bar{p}_R$ can be estimated using a material balance calculation or other reservoir model, and then k_{ro} can be determined if relative permeability data for the reservoir in question are available. The fluid properties μ_o and B_o can be obtained from a fluid sample analysis or from empirical correlations.

Once the value of $q_{o(max)}$ or J has been adjusted, future IPR's can be generated from

$$q_{o(F)} = q_{o(\max)F}\left[1 - 0.2\frac{p_{wf}}{\bar{p}_{RF}} - 0.8\left(\frac{p_{wf}}{\bar{p}_{RF}}\right)^2\right] \qquad [2.37]$$

or

$$q_{o(F)} = \frac{J_F^* p_{RF}}{1.8}\left[1 - 0.2\frac{p_{wf}}{\bar{p}_{RF}} - 0.8\left(\frac{p_{wf}}{\bar{p}_{RF}}\right)^2\right] \qquad [2.38]$$